Materials Letters 167 (2016) 242–245

Contents lists available at ScienceDirect

Materials Letters

journal homepage: www.elsevier.com/locate/matlet

Nanocrystalline carbon flakes deposited by RF magnetron sputtering

Fernando Guzmán-Olivos [a,*], Rodrigo Espinoza-González [b], Víctor Fuenzalida [a]

[a] Departamento de Física, Facultad de Ciencias Físicas y Matemáticas, Universidad de Chile, Beauchef 850, Santiago, Chile
[b] Departamento de Ciencia de los Materiales, Facultad de Ciencias Físicas y Matemáticas, Universidad de Chile, Beauchef 850, Santiago, Chile

ARTICLE INFO

Article history:
Received 5 November 2015
Received in revised form
4 January 2016
Accepted 4 January 2016
Available online 5 January 2016

Keywords:
Carbon nanoflakes
Sputtering
Carbon materials
Nanocrystalline materials

ABSTRACT

Carbon nanostructures were prepared by RF magnetron sputtering at deposition times from 30 to 120 min and temperatures on silicon substrates from 390 °C to 510 °C. Scanning and transmission electron microscopy (TEM) observations showed that carbon films deposited at 510 °C consisted of nanostructured polycrystalline carbon nanoflakes. Dark field TEM images showed carbon nanocrystals of 1 nm average size. The sp^2 hybridization decreases with increasing deposition time, as it was confirmed by X-ray photoelectron spectroscopy. The nature of these carbon nanostructures would be turbostratics, an intermediate state between hexagonal and amorphous phases.

1. Introduction

Nanostructured sheet-like carbon, also called carbon nanoflakes (CNF), consists of petal-like graphite sheets with a thickness of less than 20 nm. These nanostructures are of interest for energy storage [1], electronic [2], and biological applications [3] due to their high surface area in the order of 1000–2000 m^2/g [4], and their resistance to oxidation and high electrical conductivity [5]. Field emission cathodes based on arrays CNFs normally oriented to the substrate are considered promising materials for electrical applications [6], and can also be used in supercapacitors, since the high capacitance depends on the high specific area of conductive materials [4].

Previous works have reported the growth of CNF by hot filament chemical vapor deposition (HFCVD) [7] and by RF magnetron sputtering. In these methods, Hirase [8] proposed a growth mode of CNF related with the magnetron orientation and established that temperatures higher than 550 °C are not suitable for CNF. Zhu et al. [9] used an Ar atmosphere to grow CNF at temperatures higher than 800 °C, which has the advantage of needing neither catalytic processes nor special substrate preparation, as compared with HFCVD. This paper presents the growth of CNF by RF magnetron sputtering on silicon substrates using pure Ar plasma, but at lower temperatures than Hirase et al. [8] and Zhu et al. [9]. We study the influence of the substrate temperature and different deposition times on the carbon films.

2. Experimental procedure

Carbon films were deposited by RF magnetron sputtering using targets of pure carbon graphite (Lesker 99.999%, 50 mm in diameter). Polished silicon (100) (Silicon Quest Int.) wafers were used as substrates. The base pressure of the vacuum chamber was 3×10^{-4} Pa. Argon gas was introduced to generate plasma applying 150 W of RF-power at a constant pressure of 0.8 Pa. The films were deposited at three temperatures: 390, 460 and 510 °C using different deposition times: 30, 60, 90 and 120 min and at a constant substrate/target distance of 5 cm. The microstructure of the films was characterized by field-emission scanning electron microscopy (FESEM, FEI Inspect F50), transmission electron microscopy (TEM, FEI Tecnai F20 G^2) and X-ray Diffraction (XRD, Bruker D8 Advance with Cu Kα radiation). Samples for TEM were prepared by scraping the deposited films and placing them onto a holey carbon supported by a copper grid. The sp^2/sp^3 content of the films was determined by Raman (LabRam 010 Spectrometer, $\lambda = 633$ nm) and X-ray photoemission (XPS, Physical Electronic model 1257) spectroscopies.

3. Results and discussion

The XRD patterns (see supplementary material) of the films exhibited an amorphous character for all the conditions under study, indicating that either they are non-crystalline or the domains are smaller than the resolution of the diffractometer. FESEM images of the carbon films deposited at different temperatures during 120 min reveal various morphological structures. The films deposited at 510 °C exhibited an irregular pattern of CNF

* Corresponding author.
E-mail address: fernando.guzman@ing.uchile.cl (F. Guzmán-Olivos).

http://dx.doi.org/10.1016/j.matlet.2016.01.016
0167-577X/

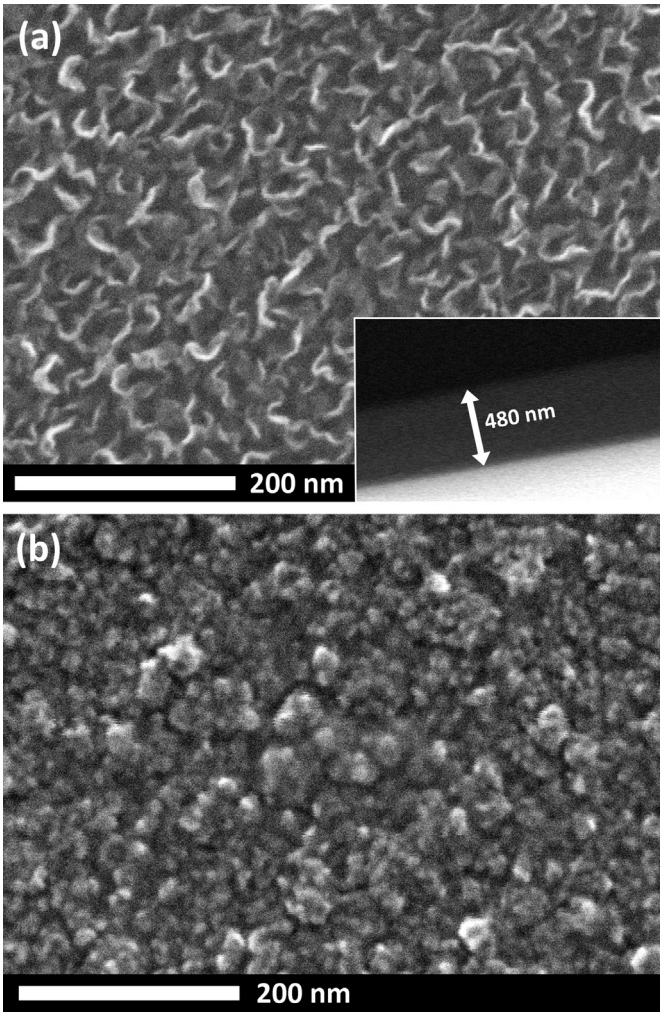

Fig. 1. FESEM image of carbon film with (a) CNF structures deposited at 510 °C during 120 min, inset image corresponds to the cross section of the film; (b) granular structures deposited at 460 °C during 120 min.

structures as it is shown in Fig. 1(a). This film consists of a large amount of clusters with leaves-shape or petals of about 100 nm size and thickness about 6 nm. The film thickness was of 480 nm, as it can be seen in the cross-sectional image depicted in the inset of Fig. 1(a). Fig. 1(b) displays a FESEM image of a film deposited at 460 °C, which has a granular microstructure of grains less than 30 nm size. Similar morphology was observed in the films deposited at 390 °C.

Fig. 2 displays TEM images of the CNF film deposited at 510 °C showing nanocrystalline graphite phases. The rings observed in the diffraction pattern (inset in Fig. 2) demonstrates the polycrystalline nature of the CNF. The broad inner ring is identified as the reflection (002) corresponding to an interplanar distance of 0.39 nm. This value is larger than the characteristic 0.34 nm reported for graphite [10], and can be associated to graphitic carbon with poor stacking order and small number of layers [11]. The other reflections were associated to the interplanar distances of 0.213 nm and 0.123 nm, and identified as the (100) and (110) graphite planes, respectively. Dark field (DF) images obtained with the (002) reflection (see Fig. 2(b)) reveal the nanocrystalline domains of the CNF with an average size of 0.9 ± 0.2 nm. These ultrafine particles observed by TEM are not suitable to be detected by XRD, due to the peak broadening produced by the size reduction of crystalline domains.

Characteristic Raman spectra of CNF films prepared under

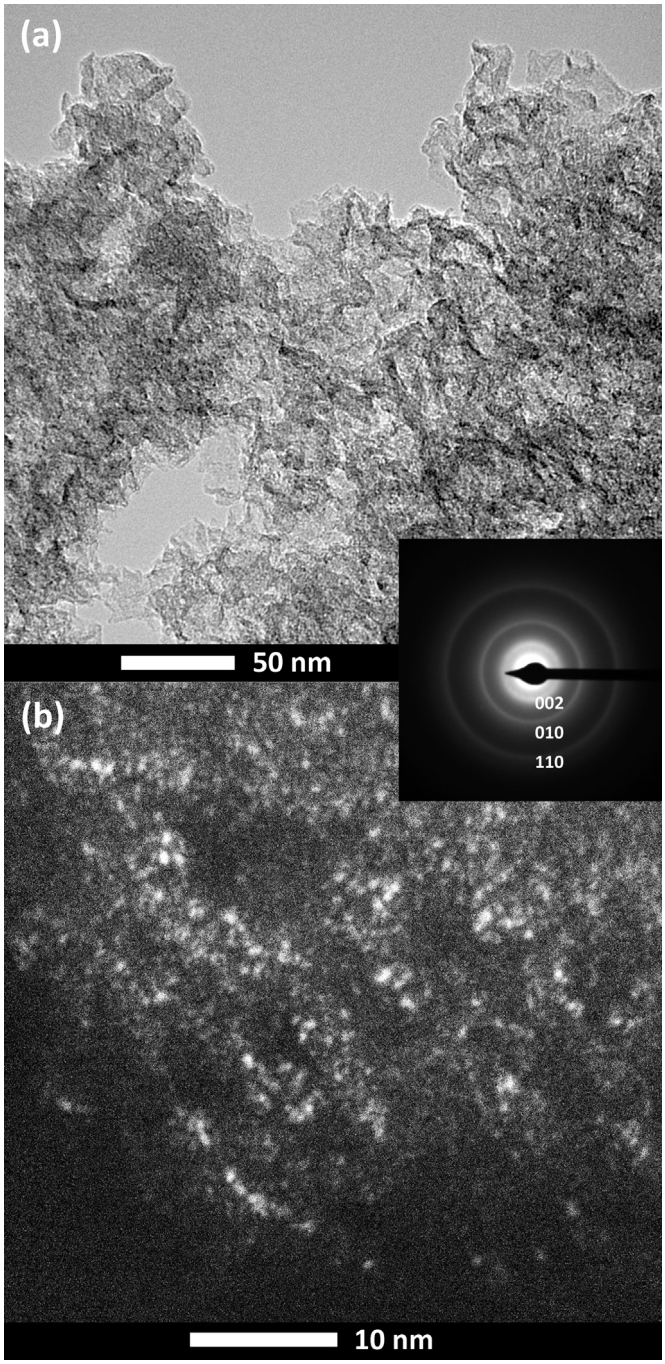

Fig. 2. TEM images of a carbon film with CNF structures deposited at 510 °C during 120 min. (a) Multibeam image, Inset SAED pattern; (b) Dark Field (DF) image showing the dimension of the nanocrystalline domains.

different deposition conditions are displayed in Fig. 3. All the spectra present the distinguishable carbon peaks, known as *D* (disorder) and *G* (graphitic) bands, which can be fitted by Lorentzian and Breit–Wigner–Fano (BWF) functions, respectively [12]. From this fit, the position of the *G* peak and the ratio between the intensities of *D* and *G* peaks, I_D/I_G, can be calculated. The values obtained the different temperatures and times of deposition are listed in Table 1. The *G* peak at 1584 cm^{-1} of the film deposited at 390 °C shifts to 1603 cm^{-1} in the film prepared at 510 °C, while the I_D/I_G ratio increases from 0.9 to 1.6 for the same samples.

It is well known that the *G* band of pristine graphite is at 1581 cm^{-1}, while the intensity of the *D* band is almost zero as well as the I_D/I_G ratio. The shift of the *G* peak to 1603 cm^{-1} in the CNF

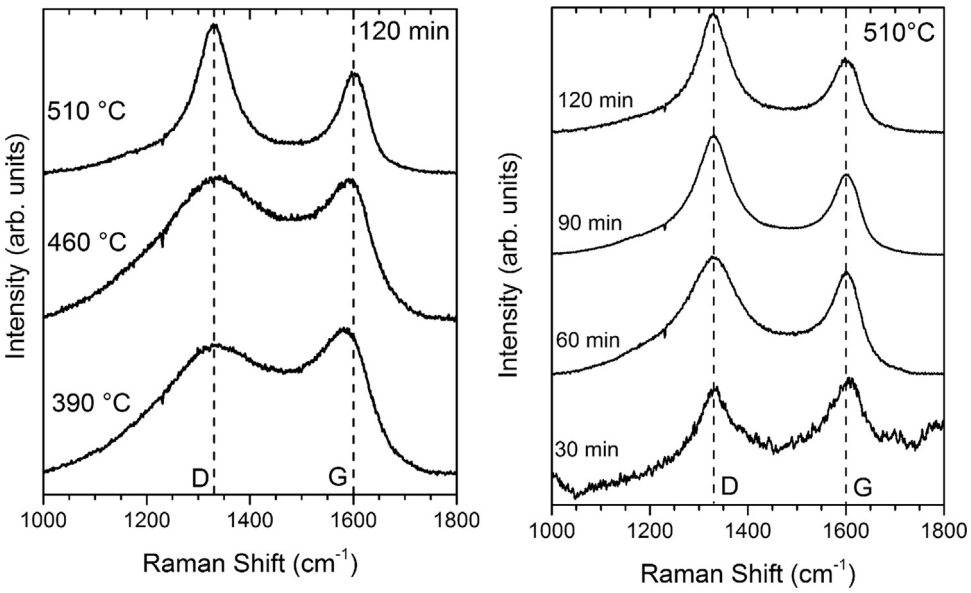

Fig. 3. Raman spectra of samples grown at different temperatures (left) and times (right). Samples with different times were grown at 510 °C.

Table 1
Deposition parameters and characteristic values calculated from Raman and XPS results (L_a calculated from (1) and sp²% is calculated from XPS fitting).

Deposition parameters (time, temperature)	G peak (cm^{-1})	I_D/I_G	L_a (nm)	sp²%
120 min–390 °C	1584	0.9	0.8	60
120 min–460 °C	1593	1.1	0.9	55
120 min–510 °C	1603	1.6	1.1	58
90 min–510 °C	1604	1.4	1.1	65
60 min–510 °C	1603	1.1	0.9	67
30 min–510 °C	1606	1.1	0.9	73

films prepared at 510 °C, and the increase in the I_D/I_G ratio are interpreted as a reduction in grain size of the ordered graphite layers [13]. This confirms the observation of nanocrystalline graphitic domains by TEM, and is consistent with the three-stage model proposed by Ferrari and Robertson [14], who proposed a quadratic model correlating the crystallite size L_a with the intensity ratio of the *D* and *G* peaks: $I_D/I_G = CL_a^2$, where *C* is a constant that depends on the excitation laser wavelength [15]. This relation was used to calculate the crystallite size value of the films prepared at the highest temperature of 510 °C, listed in Table 1. The L_a value obtained for the CNF prepared at 510 °C and 120 min of deposition is 1.1 nm, very close to the size of the nanocrystals measured from DF TEM images.

The deposition time does not affect significantly the position of the *G* peak, but the I_D/I_G ratio decreases to lower values at the shorter deposition times. This is interpreted as an increment of the amorphization associated to smaller crystalline domains according to Ferrari model [14], which supports the L_a values calculated for the carbon films prepared at lower temperatures.

Fig. 4 shows the high-resolution C 1s core level XPS spectra acquired from the CNF films grown at 510 °C at different deposition times. These spectra were fitted by four curves with maxima at 284.5, 285.4, 287.4 and 289.0 eV; the ratio of the areas of the two main fitted curves is included in Table 1. These binding energies have been assigned to chemical environments associated with C–C sp^2, C–C sp^3, C=O and O–C=O, respectively [16]. The binding energy associated to the shift between sp^2 and sp^3-hybridized carbon is 0.9 eV, similar to reported values for graphite and diamond [17]. The smaller contributions of C=O and O–C=O are attributed to the surface contamination of the samples

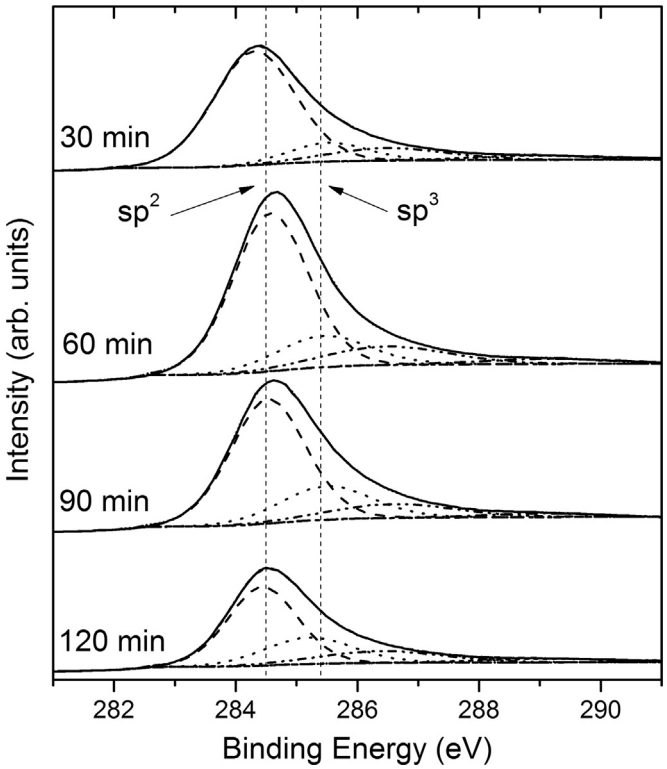

Fig. 4. High-resolution C 1s core level XPS spectra acquired from carbon films grown at 510 °C at different deposition times.

by air-exposure and from the preparation process. The sp^2 content of the CNF prepared at 510 °C and 120 min is 58%, which increases as the deposition time decreases. This analysis agrees with Raman results, where the change in the I_D/I_G ratio can be attributed to the formation of an amorphous carbon (a-C) film below the CNF for longer deposition times. This a-C film acts as a base for the formation of sp^3 hybridization according to the subplantation model of Robertson [13]; in the early deposition stages there is not enough material for sp^3 hybridization, leading to an increase of the sp^2 bonds formation for the shorter deposition times.

On the other hand, the temperature seems to have no clear

influence on the sp^2 content. The Raman measurements suggest that the shift of the *G* peak at higher temperatures would be related to a softening of the vibrational modes. The planar sp^2 clusters deposited at intermediates temperatures gradually transforms into ultrasmall turbostratic graphite type clusters that we observed as CNF at the highest deposition temperature, similar to the results of Pandiyan et al. [18]. The CNF here reported were obtained at 510 °C, which is significantly lower than the 800 °C reported by Zhu et al. [9]. Besides, Zhu deposited the CNF on Mo substrates while the silicon substrates employed in this study supports applications on microelectronic devices and field emission purposes that will be further studied. Moreover, the deposition temperature (510 °C) of the CNF is in contradiction with the minimal temperature proposed by Hirase et al. [8] for CNF growth. They suggested that the substrate temperature gives the migration energy of the carbon clusters on the substrate surface. When the substrate temperature is low, the carbon clusters have lower energy to migrate and the deposition rate becomes slower, which leads to the formation of the granular amorphous structures. While at higher temperatures, the carbon clusters from the plasma could first condense, and then grow along a direction almost normal to the substrate to form CNF [8]. Regarding this, an additional advantage of our results is the growth of CNF in the non-reactive sputtering regime reported by Hirase, which simplifies the preparation process.

4. Conclusion

We successfully developed a simple method to produce carbon nanoflakes (CNF) using RF magnetron sputtering and a carbon graphite target. The CNF were deposited on silicon substrates at lower temperatures than previous reports. A leaves-shape morphology was observed by SEM, while the ultra nanocrystalline graphitic structure in the order of one nm was confirmed by TEM and Raman spectroscopy. XPS showed that longer deposition times decrease the sp^2 content of carbon films, which was associated to the formation of an amorphous carbon (a-C) film below the CNF that acts as a base for the formation of sp^3 hybridization according to the subplantation model of Robertson. We demonstrated that the substrate temperature is a key parameter for the CNF growth.

Aknowledgements

The authors thanks to the projects Postdoctoral Fondecyt No. 3140565, Fondecyt Regular No. 1150652 and Anillo ACT1117. We also thanks to Dr. Marcos Flores for useful discussions.

Appendix A. Supplementary material

Supplementary data associated with this article can be found in the online version at http://dx.doi.org/10.1016/j.matlet.2016.01.016.

References

[1] D.J. Cott, M. Verheijen, O. Richard, I. Radu, S. De Gendt, S. Van Elshocht, et al., Synthesis of large area carbon nanosheets for energy storage applications, Carbon 58 (2013) 59–65, http://dx.doi.org/10.1016/j.carbon.2013.02.030.
[2] K.S. Novoselov, A.K. Geim, S.V. Morozov, D. Jiang, Y. Zhang, S.V. Dubonos, et al., Electric field effect in atomically thin carbon films, Science 306 (2004) 666–669, http://dx.doi.org/10.1126/science.1102896.
[3] R. Vansweevelt, A. Malesevic, M. Van Gompel, A. Vanhulsel, S. Wenmackers, J. D'Haen, et al., Biological modification of carbon nanowalls with DNA strands and hybridization experiments with complementary and mismatched DNA, Chem. Phys. Lett. 485 (2010) 196–201, http://dx.doi.org/10.1016/j.cplett.2009.12.040.
[4] X. Zhao, H. Tian, M. Zhu, K. Tian, J.J. Wang, F. Kang, et al., Carbon nanosheets as the electrode material in supercapacitors, J. Power Sources 194 (2009) 1208–1212, http://dx.doi.org/10.1016/j.jpowsour.2009.06.004.
[5] Y.H. Wu, T. Yu, Z.X. Shen, Two-dimensional carbon nanostructures: fundamental properties, synthesis, characterization, and potential applications, J. Appl. Phys. 108 (2010) 071301, http://dx.doi.org/10.1063/1.3460809.
[6] W.C. Shih, J.M. Jeng, C.T. Huang, J.T. Lo, Fabrication of carbon nanoflakes by RF sputtering for field emission applications, Vacuum 84 (2010) 1452–1456, http://dx.doi.org/10.1016/j.vacuum.2010.01.049.
[7] N.G. Shang, F.C.K. Au, X.M. Meng, C.S. Lee, I. Bello, S.T. Lee, Uniform carbon nanoflake films and their field emissions, Chem. Phys. Lett. 358 (2002) 187–191, http://dx.doi.org/10.1016/S0009-2614(02)00430-X.
[8] Y. Hirase, Y. Ichikawa, Growth mode of CNFs on substrates by using the sputtering method, IEEJ Trans. Electr. Electron. Eng. 7 (2012) 334–336, http://dx.doi.org/10.1002/tee.21736.
[9] D.M. Zhu, G. Jakovidis, L. Bourgeois, Catalyst-free synthesis of carbon and boron nitride nanoflakes using RF-magnetron sputtering, Mater. Lett. 64 (2010) 918–920, http://dx.doi.org/10.1016/j.matlet.2010.01.058.
[10] H.O. Pierson, Handbook of Carbon, Graphite, Diamonds and Fullerenes, Noyes Publications, Park Ridge, New Jersey, USA (1993) http://dx.doi.org/10.1016/B978-0-8155-1339-1.50008–6.
[11] L. Pauling, The structure and properties of graphite and boron nitride, Proc. Natl. Acad. Sci. USA 56 (1966) 1646–1652, http://dx.doi.org/10.1073/pnas.56.6.1646.
[12] S. Prawer, K.W. Nugent, Y. Lifshitz, G.D. Lempert, E. Grossman, J. Kulik, et al., Systematic variation of the Raman spectra of DLC films as a function of sp^2: sp^3 composition, Diam. Relat. Mater. 5 (1996) 433–438.
[13] J. Robertson, Diamond-like amorphous carbon, Mater. Sci. Eng. R Rep. 37 (2002) 129–281, http://dx.doi.org/10.1016/S0927-796X(02)00005-0.
[14] A.C. Ferrari, J. Robertson, Interpretation of Raman spectra of disordered and amorphous carbon, Phys. Rev. B 61 (2000) 14095–14107, http://dx.doi.org/10.1103/PhysRevB.61.14095.
[15] L.G. Cançado, K. Takai, T. Enoki, M. Endo, Y. a Kim, H. Mizusaki, et al., General equation for the determination of the crystallite size L_a of nanographite by Raman spectroscopy, Appl. Phys. Lett. 88 (2006) 1–4, http://dx.doi.org/10.1063/1.2196057.
[16] J.I. Wilson, J. Walton, G. Beamson, Analysis of chemical vapour deposited diamond films by X-ray photoelectron spectroscopy, J. Electron Spectrosc. Relat. Phenom. 121 (2001) 183–201, http://dx.doi.org/10.1016/S0368-2048(01)00334-6.
[17] R. Haerle, E. Riedo, A. Pasquarello, A. Baldereschi, sp^2/sp^3 hybridization ratio in amorphous carbon from C 1s core-level shifts: x-ray photoelectron spectroscopy and first-principles calculation, Phys. Rev. B 65 (2001) 32–37, http://dx.doi.org/10.1103/PhysRevB.65.045101.
[18] R. Pandiyan, N. Delegan, a Dirany, P. Drogui, M. a El Khakani, Correlation of sp^2 carbon bonds content in magnetron-sputtered amorphous carbon films to their electrochemical H_2O_2 production for water decontamination applications, Carbon 94 (2015) 988–995, http://dx.doi.org/10.1016/j.carbon.2015.07.071.